Estimating Fuel Characteristics from Simulated Circulating Fluidized Bed Furnace Data

Markus Neuvonen
Intelligent Machines and Systems
University of Oulu
Oulu, Finland
markus.neuvonen@oulu.fi

István Selek
Intelligent Machines and Systems
University of Oulu
Oulu, Finland
istvan.selek@oulu.fi

Enso Ikonen
Intelligent Machines and Systems
University of Oulu
Oulu, Finland
enso.ikonen@oulu.fi

***Abstract*—This paper proposes a soft sensor to estimate the elementary fuel characteristics in combustion–thermal power plants. The proposed approach is data–driven. The input–output data is generated by a digital twin. Application targets circulating fluidized bed boiler, where furnace (combustion) side is considered only. First, the nonlinear dynamics of the furnace is approximated with a linear time–invariant dynamic model. Then two separate methods, Kalman filter and internal governor, are applied for state estimation. Results show that the approach is viable and has low computational complexity, but the weakly observable modes are difficult to predict accurately.**

***Index Terms*—linear and nonlinear systems, estimations and identification, monitoring and diagnostics**

A. Nomenclature

Set of real numbers and positive integers are denoted by $\mathbb{R}$, and $\mathbb{Z}_+$ respectively. Vectors (matrices) appear using bold regular $\mathbf{x}$ (bold capital $\mathbf{M}$) typeset. Symbols $(.)^T$, $(.)^{-1}$ and $(.)^\dagger$, represent transposition operator, inverse and Moore–Penrose pseudoinverse.

I. Introduction

The Circulating Fluidized Bed (CFB) technology is the mainstream of the industrial combustion–thermal power plant installations. They are well suited for combusting solid fuels of varying quality with high combustion efficiency [1]. Their working principle is to continuously mix bed materials and fuel feed with strong upward airflow, which separates the solid particles and gives the mixture desired fluid–like combustion properties. Recirculation of solid particles from flue gas path back to furnace further increases combustion efficiency.

Fuel characteristics and furnace conditions determine the properties of the resulting flue gas. The thermal energy of flue gas is rejected to water–steam cycle by heat exchangers located in flue gas duct. Simultaneously harmful particles from combustion can cause fouling and corrosion on these surfaces. This phenomenon has a significant impact on the heat–to–power conversion efficiency of the power plant, as it reduces the efficiency of heat transfer and degrades the life expectancy of the equipment. The decay of efficiency has extreme importance in industrial applications, and the outlined problem has been studied extensively in the literature. Efficiency loss can be controlled with knowledge of fuel characteristics [2], [3]. Fuel characteristics can be determined via laboratory experiments, and they are well defined for standard fuels [4], [5].

The importance of *fuel flexibility* (ability to change fuel type in a short time frame) is increasing and dominates the industrial trends. Various waste–derived fuels are becoming more and more integral part of the thermal power plant fuel palette. However, it is highly unusual for an industrial plant to be equipped with online, in–situ measurement of the fuel composition. For example, in industrial waste fuel thermal plants, fouling and corrosion–related issues are typically handled by merely avoiding fuel quality variations; persistent waste fuel type mixed with appropriate fossil fuel or additives are used [6]–[8].

Despite the importance of the topic, according to the best of the authors' knowledge, very few tools exist for online measurement of fuel characteristics. Some examples are near–infrared–, and hot air drying sensors [9], [10]. To address the aforementioned challenges, a promising alternative is the so–called *soft sensor* approach (computationally estimating unknown process conditions based on existing measurements). In case the underlying process model is dynamic, the soft sensor can be stated as a state–estimation problem. For example, [11] and [12] developed soft sensors for the estimation of fuel moisture content.

This paper develops a soft sensor to estimate the fuel characteristics in combustion–thermal CFB power plant application. The soft sensor is data–driven and computationally tractable. First, a linear time-invariant (LTI) approximation of nonlinear furnace dynamics is achieved with subspace identification method. Then two separate methods for estimating the fuel characteristics are applied and their estimation results compared. All Input–Output (IO) data in this research is generated by a *digital twin* (a mathematical model of the physical plant) of the CFB boiler furnace.

This work was conducted in the H2020 project COGNITWIN (grant number 870130).

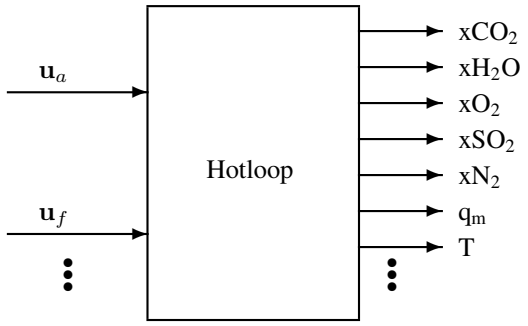

Fig. 1. The input–output structure of the furnace model. Vector $\mathbf{u}_a \in \mathbb{R}^2$ contains primary– and secondary air flows to furnace, vector $\mathbf{u}_f \in \mathbb{R}^7$ includes the elementary chemical composition of the fuel. The outputs are measured at the discharge port of the furnace (intake of the flue–gas path), consisting of flue gas mass flow q_m, –temperature T and –concentrations of CO_2, H_2O, O_2, SO_2 and N_2.

The paper is organized as follows: Section II presents how LTI system presentation was obtained from IO–data. Section III implements Kalman Filter soft sensor, whereas Section IV uses internal governor approach. Section V summarizes the results and discusses needs for future development.

II. System Identification

The development of soft sensors for the estimation of fuel characteristics is based on dynamic model that captures the dominant dynamics of the process of interest. The modeling approach adopted by this paper is data–driven, that is, the mathematical representation is constructed in a black–box fashion, using only input–output data.

Due to lack of real power plant field measurements, the IO data used for soft sensor development is synthetic and generated by a digital twin. The digital twin used in this work is property of Sumitomo SHI FW Energia Oy and known under the name Hotloop [13], [14]. Hotloop is a first–principle (white–box) model developed in–house for representing the combustion dynamics of a CFB furnace. It is extensively used in the design and analysis of CFB power plants by the owner and is considered reliable in capturing dynamic and steady–state performance.

Inherently, the Hotloop is highly nonlinear with more than hundred input– and output signals. The magnitude of the dimension of its state–space is 10^3. Hotloop is implemented in MATLAB Simulink environment, and its analytical, digital representation is hidden from the user.

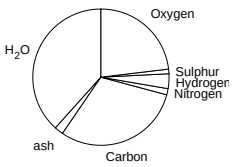

Fig. 2. An example of characteristics of some fuel. Any fuel can be partitioned into its characteristics. Partitioning is defined by input vector $\mathbf{u}_f \in \mathbb{R}^7$.

For identification, we only consider the most relevant combustion related input signals and flue gas properties as outputs which are obtainable (measured, observed) in real installations. In what follows, a total of nine input– and seven output signals were recorded during the digital experiments. The IO structure of the CFB furnace model is depicted in Fig. 1.

The input space is partitioned into air and fuel subspaces represented by vectors $\mathbf{u}_a \in \mathbb{R}^2$ and $\mathbf{u}_f \in \mathbb{R}^7$. The input sequence generated in the outlined subspaces must respect the following constraints: $\mathbf{u}_{a,k} \in \{\mathbf{u}_a^{\text{high}}, \mathbf{u}_a^{\text{low}}\}$ and

$$u_{f,i}^{\min} \leq u_{f,i,k} \leq u_{f,i}^{\max}, \quad \sum_{i=1}^{7} u_{f,i,k} = 1 \tag{1}$$

for all $k = 0, 1, \ldots$ where $u_{f,i,k}$ denotes the mass fraction of ith fuel component ($i \in \{1, \ldots, 7\}$) at time k. Figure 2 depicts the fuel composition constraint while Table I quantifies the "box" constraints for air– and fuel feeds respectively.

A. IO data collection

System identification begins with the generation of the input sequence and continues with the collection of simulated output data. The identification approach requires that the generated input sequence satisfies the persistently exciting condition to be able to capture the dynamical behavior of the model by input–output experiments. To achieve this, the input sequence was generated by a random walk in the air feed and fuel characteristics subspaces subject to the outlined constraints. For the air feed this means a random binary sequence generated by a coin flipping strategy with fifty–fifty percent probability for each possible event ($\{\mathbf{u}_a^{\text{high}}, \mathbf{u}_a^{\text{low}}\}$) to occur.

For the fuel characteristics, the input sequence is generated by the recursion

$$\mathbf{u}_{f,k+1} = \lfloor \mathbf{u}_f^{\min}, \mathbf{u}_{f,k} + \mathbf{A}\boldsymbol{\alpha}_k, \mathbf{u}_f^{\max} \rceil, \;\; \mathbf{u}_{f,0} = \mathbf{u}_f^{\star} \tag{2}$$

where $\mathbf{u}_f^{\star}$ is a pre–defined steady input representing a nominal fuel composition subject to constraints, the columns of matrix $\mathbf{A}$ are orthonormal basis vectors of the nullspace of $\mathbf{e}_7 := [1\,1\,1\,1\,1\,1\,1]^T$ and $\boldsymbol{\alpha}_k \in \mathbb{R}^6$ is a random vector. Its components are generated by sampling the continuous uniform distribution in a close proximity of the origin, that is, $\alpha_{i,k} \sim \mathcal{U}_{[-\delta,\delta]}$, $\delta \in \mathbb{R}_+$ is a "small" parameter for all

TABLE I
Used input variables and their limits

	Furnace variables[a] $[kg/s]$						
	Primary air			***Secondary air***			
High	34.0			20.0			
Low	32.3			19.0			
	Fuel characteristics[b] $[-]$						
	H_2O	***ash***	***C***	***H***	***N***	***S***	***O***
Max	0.60	0.1	0.60	0.1	0.1	0.1	0.30
Min	0.25	0	0.25	0	0	0	0.15

[a]Either High or Low. These form input vector $\mathbf{u}_a$.
[b]Between Min and Max. These form input vector $\mathbf{u}_f$.

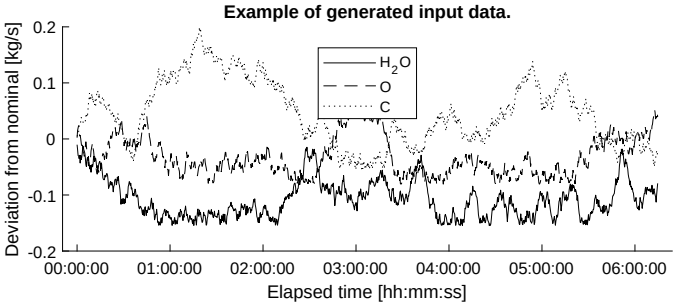

Fig. 3. Example of generated random walk input to Hotloop.

$i \in \{1, \ldots, 6\}$ and $k = 0, 1, \ldots$ ($\alpha_{i,k}$ are uncorrelated in both spatial and temporal dimensions).

The function $\lfloor \mathbf{x}^{\min}, \mathbf{x}, \mathbf{x}^{\max} \rceil$, $\mathbf{x}^{\min} = [x_1^{\min}, \ldots, x_n^{\min}]^T \in \mathbb{R}^n$, $\mathbf{x} = [x_1, \ldots, x_n]^T \in \mathbb{R}^n$, $\mathbf{x}^{\max} = [x_1^{\max}, \ldots, x_n^{\max}]^T \in \mathbb{R}^n$ represents vectorial saturation, that is

$$\lfloor \mathbf{x}^{\min}, \mathbf{x}, \mathbf{x}^{\max} \rceil := \begin{cases} x_i^{\min} & \text{if} \quad x_i < x_i^{\min} \\ x_i & \text{if} \quad x_i^{\min} \leq x_i \leq x_i^{\max} \\ x_i^{\max} & \text{if} \quad x_i > x_i^{\max} \end{cases} \tag{3}$$

for all $i = 1, \ldots, n$.

Using the generated persistently exciting input sequence $[\mathbf{u}_{a,k}, \mathbf{u}_{f,k}]^T$, the digital twin's output response $\mathbf{y}_k$ was recorded using a 20 sec sampling time on a long–enough lookahead horizon. The output signal obtained by simulation is noiseless. As measurement deviations are in scale 10^2 for temperature and 10^{-2} for concentrations, they are all scaled to magnitude 10^0 for equal importance in identification.

The simulation of the IO response was initiated from a steady state IO condition corresponding to the $([\mathbf{u}_a^\star, \mathbf{u}_f^\star]^T, \mathbf{y}^\star)$ pair. For identification the excited dynamics around the outlined steady state was considered which is represented by the $([\mathbf{u}_{a,k} - \mathbf{u}_a^\star, \mathbf{u}_{f,k} - \mathbf{u}_f^\star]^T, \mathbf{y}_k - \mathbf{y}^\star)$ IO data pair. For example, input data of three different fuel characteristics used for identification is shown in Figure 3.

B. LTI model identification

We now have a set of data with m inputs and p outputs. Subspace identification method MOESP is well suited for model identification directly from deterministic multiple–input multiple–output data [15]. The applied computational algorithm for MOESP is presented in [16].

Following the MOESP algorithm, a finite set of Hankel matrices can be made from obtained data set. Different data matrices follow from heuristic selection of parameters $n \in \mathbb{Z}_+$ (the number of system states), $l \in \mathbb{Z}_+$ (the size of extended observability matrix $\boldsymbol{\mathcal{O}}_l = \begin{bmatrix} \mathbf{C} & \mathbf{CA} & \ldots & \mathbf{CA}^{l-1} \end{bmatrix}^T$), and $N \in \mathbb{Z}_+$ (the size of extended controllability matrix $\boldsymbol{\mathcal{C}}_N = \begin{bmatrix} \mathbf{B} & \mathbf{AB} & \ldots & \mathbf{A}^{N-1}\mathbf{B} \end{bmatrix}$).

The state dimensions can be freely chosen, f.ex. $n \in \{2, 3, \ldots, 20\}$. The extended observability matrix must be strictly bigger than state dimension ($l > n$) and Hankel matrix is recommended to have at least twice as many columns (l) as rows (mN and pN for input- and output Hankels respectively) for MOESP subspace identification. With different combinations, a few hundred different LTI system realizations are found. To select the most suitable model from the set of found realizations, following criteria is used:

- model is stable, i.e. $\max \|\lambda(\mathbf{A})\| < 1$, where function $\lambda(.)$ returns eigenvalues of argument matrix,
- system is numerically observable, i.e. $\min \sigma(\boldsymbol{\mathcal{O}}) > 10^{-6}$, where function $\sigma(.)$ returns singular values of argument matrix, and
- produces the most accurate LTI–model outputs $\hat{\mathbf{y}}$, i.e. minimizes $\sum \|\mathbf{y}_k - \hat{\mathbf{y}}_k\|$

With this data and criteria, we selected LTI model with seven state dimensions. Even with such low dimension of state space (which is beneficial for computational reasons), the input–output dynamics of found LTI model are visually indistinguishable compared to original data (Fig. 4). However, with further numerical analysis it can be noted that the estimation is biased, see for example Fig. 5. At later stages of soft sensor development this bias may prove to be a problem.

III. KALMAN FILTER

Having identified the LTI system, we would now like to use it for estimating system inputs $\mathbf{u}_f$. Kalman Filter is well established method of estimating unknown states of a system

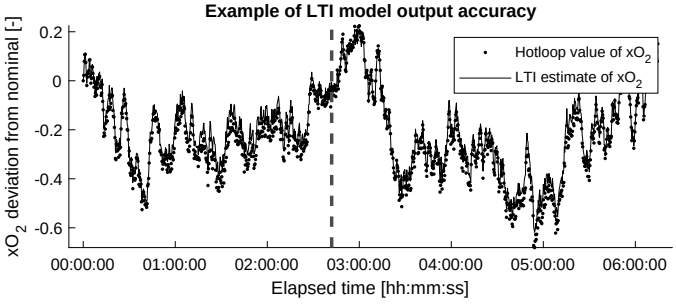

Fig. 4. Comparison of one Hotloop and LTI-model output. The dashed vertical line indicates amount of data (starting from time 0) was used is subspace identification of selected model.

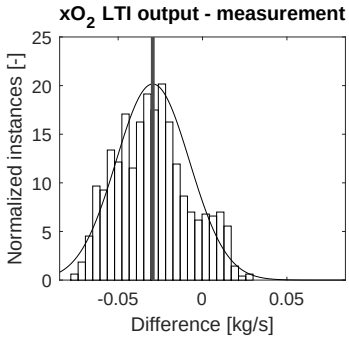

Fig. 5. The statistical distribution of the error between the measured and LTI model output xO_2. Normal distribution curve has been fitted to the data, and mean is marked with vertical line.

with only measurement data, no state information is needed. To implement it, we need to augment the inputs of interest into the states of the system, as done in (4). Note, we have omitted the negligible $\mathbf{D}$ matrix.

$$\begin{bmatrix} \mathbf{x}_{k+1} \\ \mathbf{u}_{f,k+1} \end{bmatrix} = \begin{bmatrix} \mathbf{A} & \mathbf{B}_f \\ \mathbf{0} & \mathbf{I} \end{bmatrix} \begin{bmatrix} \mathbf{x}_k \\ \mathbf{u}_{f,k} \end{bmatrix} + \begin{bmatrix} \mathbf{B}_a \\ \mathbf{0} \end{bmatrix} \mathbf{u}_{a,k}$$
$$\hat{\mathbf{y}}_k = \begin{bmatrix} \mathbf{C} & \mathbf{0} \end{bmatrix} \begin{bmatrix} \mathbf{x}_k \\ \mathbf{u}_{f,k} \end{bmatrix} \tag{4}$$

where we have used $\mathbf{u} = \begin{bmatrix} \mathbf{u}_a & \mathbf{u}_f \end{bmatrix}^T$ and, correspondingly $\mathbf{B} = \begin{bmatrix} \mathbf{B}_a & \mathbf{B}_f \end{bmatrix}$. Augmentation requires an assumption of state dynamics, we have used identity matrix $\mathbf{I}$ to achieve accurate steady–state ($\mathbf{u}_{f,k+1} = \mathbf{u}_{f,k}$).

As was seen in Fig. 5, the LTI estimation of original nonlinear system is biased. Even though Kalman Filter is constructed on the assumption of zero–mean errors, the biased error would not cause significant estimation error for systems with high degree of observability. But low degree of observability magnifies the bias into large estimation error. In this case, the augmented system (4) has lowest observability gramian singular value in the magnitude 10^{-7}, and the second lowest in 10^{-3}, making Kalman Filter very sensitive to bias.

The results of fuel characteristics estimation with soft sensor implementing Kalman Filter are shown in Fig. 6. Error of estimation is defined as $\mathbf{u}_{f,k} - \hat{\mathbf{u}}_{f,k}$ and presented as percentage compared to total deviation in the value of each fuel characteristic ($\max\{u_{i,1}, \ldots, u_{i,N}\} - \min\{u_{i,1}, \ldots, u_{i,N}\}$). With visual inspection some inputs are estimated well, but sensitivity to weakly observable subspace is confirmed.

IV. Internal Governor

Also another fuel characteristics estimation method, based on internal governor, is proposed for soft sensor implementation. It will use full state information, but is expected to handle biased model error. Idea is to find such fuel characteristics input vector that matches the LTI model outputs to measured outputs. The implementation follows these steps:

1) Augment the state of identified model with integrator.
2) Create closed–loop state controller using fuel characteristics as feedback.
3) Find proper gain matrix $\mathbf{K}$ for state feedback.

Augmenting the state space with integrator dynamics guarantees reaching of reference value in steady–state, assuming the system is stable. We introduce additional state vector $\mathbf{z}$ and modify the state space model in such a way that in steady–state the LTI-model output vector $\hat{\mathbf{y}} = \mathbf{C}\mathbf{x}$ is equal to the output obtained from Hotloop simulation $\mathbf{y}$ (i.e. the reference for the integrator), as in (5).

$$\begin{bmatrix} \mathbf{x}_{k+1} \\ \mathbf{z}_{k+1} \end{bmatrix} = \underbrace{\begin{bmatrix} \mathbf{A} & \mathbf{0} \\ -\mathbf{C} & \mathbf{I} \end{bmatrix}}_{\tilde{\boldsymbol{A}}} \underbrace{\begin{bmatrix} \mathbf{x}_k \\ \mathbf{z}_k \end{bmatrix}}_{\tilde{\boldsymbol{x}}_k} + \begin{bmatrix} \mathbf{B}_a \\ \mathbf{0} \end{bmatrix} \mathbf{u}_{a,k} + \underbrace{\begin{bmatrix} \mathbf{B}_f \\ \mathbf{0} \end{bmatrix}}_{\tilde{\boldsymbol{B}}} \mathbf{u}_{f,k} + \begin{bmatrix} \mathbf{0} \\ \mathbf{I} \end{bmatrix} \mathbf{y}_k$$
$$\hat{\mathbf{y}}_k = \begin{bmatrix} \mathbf{C} & \mathbf{0} \end{bmatrix} \begin{bmatrix} \mathbf{x}_k \\ \mathbf{z}_k \end{bmatrix} \tag{5}$$

Internal governor approach is based on taking steady–state input vector $\mathbf{u}^*_{f,k}$ as fuel characteristics estimate. This obviously makes sense only if the steady–state input vector $\mathbf{u}^*_{f,k}$ is unique. Uniqueness can be verified by solving LTI system for steady–state, i.e. $\mathbf{x}_{k+1} = \mathbf{x}_k$, which leads to linear problem of format (6).

$$\mathbf{u}^*_{f,k} = (\mathbf{C}(\mathbf{I} - \mathbf{A})^{-1}\mathbf{B}_f)^\dagger \mathbf{b} \tag{6}$$

, where vector $\mathbf{b} = \hat{\mathbf{y}}_k - \mathbf{C}(\mathbf{I} - \mathbf{A})^{-1}\mathbf{B}_a\mathbf{u}_{a,k}$.

If the rank of the pseudoinversed matrix equals the size of unknown vector, the solution is unique. For this application this condition is satisfied, and we can proceed. The smallest eigenvalue is in magnitude 10^{-5}, though, reflecting the continuing difficulty of weak observability.

Next we will close the loop by implementing static state feedback. The controlled input will be the fuel characteristics input vector $\mathbf{u}_{f,k} = \begin{bmatrix} \mathbf{K}_1 & \mathbf{K}_2 \end{bmatrix} \tilde{\boldsymbol{x}}_k$, where matrix $\mathbf{K}$ is the state gain matrix. It is divided into two segments (with respect to original state variables and the new integrator variables) for notational clarity. When this is inserted into (5), we get (7).

$$\begin{bmatrix} \mathbf{x}_{k+1} \\ \mathbf{z}_{k+1} \end{bmatrix} = \begin{bmatrix} \mathbf{A} + \mathbf{B}_f\mathbf{K}_1 & \mathbf{B}_f\mathbf{K}_2 \\ -\mathbf{C} & \mathbf{I} \end{bmatrix} \begin{bmatrix} \mathbf{x}_k \\ \mathbf{z}_k \end{bmatrix} \cdots + \begin{bmatrix} \mathbf{B}_a \\ \mathbf{0} \end{bmatrix} \mathbf{u}_{a,k} + \begin{bmatrix} \mathbf{0} \\ \mathbf{I} \end{bmatrix} \mathbf{y}_k$$
$$\hat{\mathbf{y}}_k = \begin{bmatrix} \mathbf{C} & \mathbf{0} \end{bmatrix} \begin{bmatrix} \mathbf{x}_k \\ \mathbf{z}_k \end{bmatrix} \tag{7}$$

The final task is to choose the matrix $\mathbf{K}$ in such way that the homogenous part of integrator augmented closed–loop system is stable. This can be achieved by pole placement method. We perform similarity transformation with matrix $\mathbf{T}$ to obtain diagonal matrix $\mathbf{\Lambda}$, where the diagonal values are the set (stable) poles of the closed–loop system (8).

$$\boldsymbol{T}^{-1}(\tilde{\boldsymbol{A}} + \tilde{\boldsymbol{B}}\boldsymbol{K})\boldsymbol{T} = \mathbf{\Lambda} \tag{8}$$

where $\tilde{\mathbf{A}}$ and $\tilde{\mathbf{B}}$ are given, $\mathbf{\Lambda}$ contains the set poles, $\boldsymbol{K}$ can be freely selected and $\boldsymbol{T}$ is the unknown.

With respect to the unknown matrix $\boldsymbol{T}$, (8) can be written in Sylvester equation form (9).

$$\tilde{\boldsymbol{A}}\boldsymbol{T} - \boldsymbol{T}\mathbf{\Lambda} = -\tilde{\boldsymbol{B}} \underbrace{\boldsymbol{K}\boldsymbol{T}}_{\boldsymbol{G}} \tag{9}$$

where matrix $\mathbf{G}$ can be chosen arbitrarily.

Sylvester equation (9) will have an invertible solution $\mathbf{T}$ if and only if the following conditions are satisfied:

- ($\tilde{\boldsymbol{A}}$,$\tilde{\boldsymbol{B}}$) is controllable.
- ($\mathbf{\Lambda}$,$\boldsymbol{G}$) is observable.
- $\tilde{\boldsymbol{A}}$ and $\mathbf{\Lambda}$ have no common eigenvalues.

The first condition can be added as selection criteria when choosing the most suitable LTI model in identification stage, the latter two can be checked while selecting the set pole locations $\mathbf{\Lambda}$ and the arbitrary matrix $\boldsymbol{G}$.

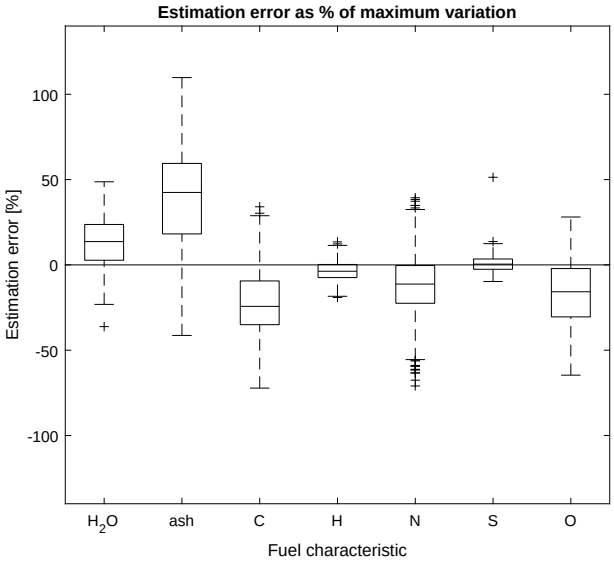

Fig. 6. Soft sensor performance with Kalman Filter on test data set. For each characteristic, 25th and 75th percentile of error variation are lower- and upper edges of the box, center line of the box is the median, extreme errors are marked as whiskers, and possible outliers as separate crosses.

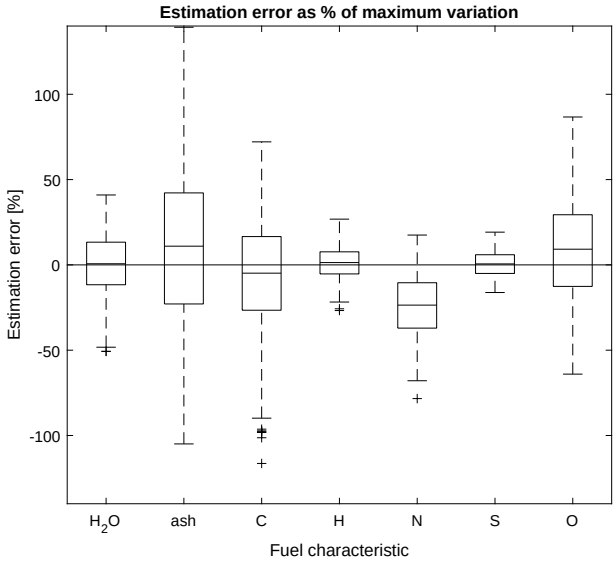

Fig. 7. Soft sensor performance with internal governor procedure on test data set. 25th and 75th percentile, median, extreme points and outliers are marked as in Fig. 6.

When solution to Sylvester equation is found, static state feedback gain $\boldsymbol{K}$ can be directly back calculated from $\boldsymbol{K} = \boldsymbol{G}\boldsymbol{T}^{-1}$ (found $\boldsymbol{T}$ is known to be invertible) and state space presentation of (7) can be completed.

Closed–loop system's dominant time–constant is set to be smaller than simulation timestep (sampling time). Therefore $\tilde{\boldsymbol{x}}_{k+1} = \tilde{\boldsymbol{x}}_k$ for internal governor soft sensor within each step k. The used fuel characteristics input $\mathbf{u}_{f,k} = \boldsymbol{K}\tilde{\boldsymbol{x}}_k$ is recorded as the soft sensor output.

Soft sensor performance of estimating fuel characteristics with internal governor on verification data is shown in Fig. 7. This is the same visualization as was done for implementation with Kalman Filter earlier in Fig. 6. Clearly better mean value for estimation is reached, while standard deviation has increased slightly; values for these statistical parameters are presented in Table II for comparison. Soft sensor performance continues to vary for different characteristics, following the observability of modes. A section of verification data and corresponding internal governor –method estimates for all seven fuel characteristics is shown in Fig. 8.

V. Summary

In this paper, a soft sensor for estimating the elementary chemical composition of the combusted fuel in thermal power plant was developed. The application was a circulating fluidized bed furnace. Subspace identification method was applied to approximate the (nonlinear) combustion dynamics with a linear time–invariant system from IO–data. Then two separate methods were used to complete the soft sensor:

1) Kalman filter approach: Reformulate the obtained LTI model by augmenting the elementary chemical composition of fuel from model inputs to model states, state estimate with the augmented model.
2) Internal governor approach: Reformulate the obtained LTI model by augmenting an integrator and static state controller. Find the unique fuel input that produces the measured outputs and use it as the estimate.

Proposed fuel characteristics soft sensors were tested with simulated data. All simulations were noiseless. Kalman Filter approach was seen to be inaccurate due to biased modeling error magnification by weak observability. Internal governor approach was able to produce better results in visual inspection, but same curse of weak observability was still seen.

For practical plant operation purposes, the overall high/low trend information of fuel characteristics is sufficient. Fuel characteristics can be estimated within trend accuracy with the proposed soft sensors. Sufficiently accurate results are produced in simulation environment. Further analysis of establishing the criteria for choosing the best LTI state space model representation could improve performance of proposed soft sensor.

Estimation of fuel characteristics can be used to minimize the undesired, power plant efficiency reducing phenomena. Future plan is to apply this method online in real plant. This online estimator is envisioned to rely on subspace identification procedure of Hotloop simulated data with similar process conditions as the plant is currently running in. Outstanding problems for such application include taking

TABLE II
Means and standard deviations of fuel characteristics estimation error in Kalman Filter– and internal governor approaches.

	H_2O	ash	C	H	N	S	O
KF mean	0.35	0.42	-0.31	-0.04	-0.13	0.01	-0.27
IG mean	0.00	0.11	-0.08	0.01	-0.26	0.01	0.16
KF std	0.37	0.31	0.27	0.06	0.19	0.05	0.31
IG std	0.46	0.51	0.46	0.09	0.19	0.08	0.48

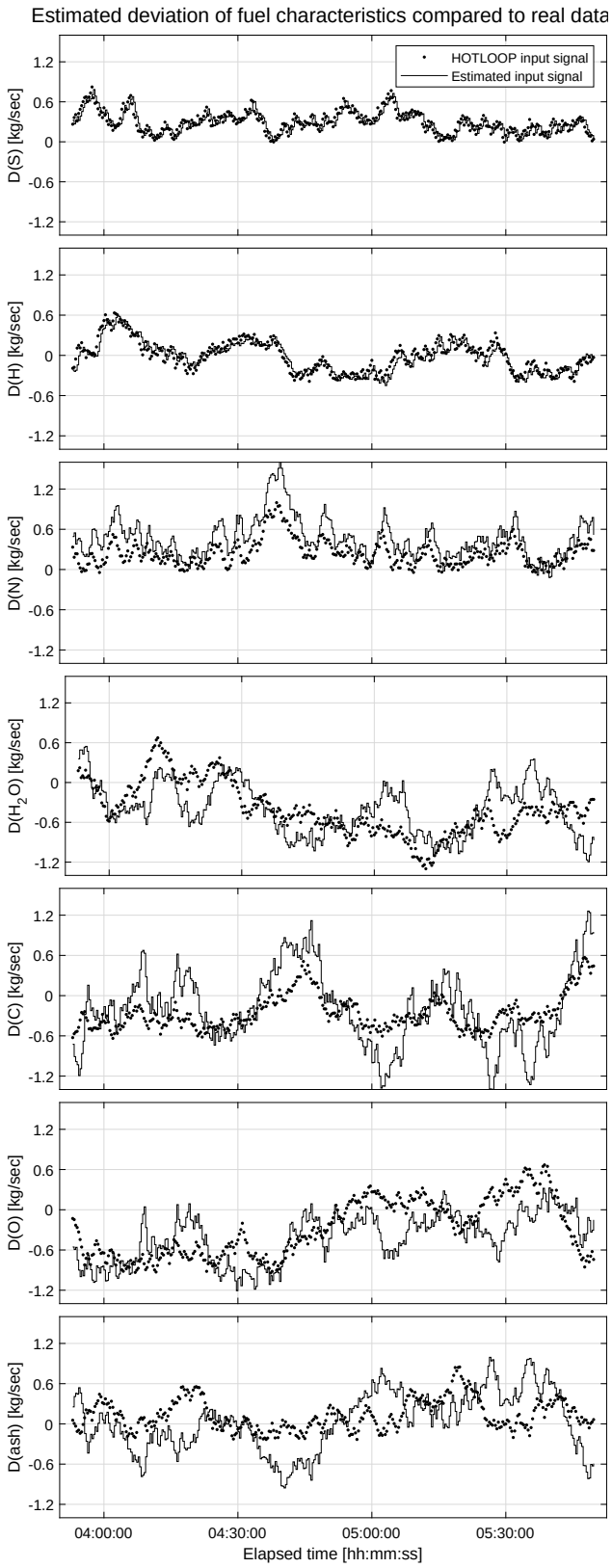

Fig. 8. The real- and estimated value of the seven fuel characteristic sorted from most accurate to least accurate.

measurement noise characteristics into account and matching the measurements points of the plant and the simulator from both software– and instrumentation hardware point–of–view.

REFERENCES

[1] Makkonen, P., "Foster Wheeler CFB with the New INTREX™ Superheater," VGB POWERTECH, Volume 80, Issue 2, pp.30–34, 2000.

[2] Richard W. Bryers, "Fireside slagging, fouling, and high-temperature corrosion of heat-transfer surface due to impurities in steam-raising fuels," Progress in Energy and Combustion Science, Volume 22, Issue 1, pp. 29–120, 1996.

[3] L-E. A.Mand, B. Leckner, "The role of fuel volatiles for the emission of nitrogen oxides from fluidized bed boilers a comparison between designs," Twenty-Third Symposium (International) on Combustion, pp. 927–933, 1990.

[4] Piispanen M.H.,Niemela M.E.,Tiainen M.S.,Laitinen R.S., "Prediction of bed agglomeration propensity directly from solid biofuels: A look behind fuel indicators," Energy and Fuels, Volume 26, Issue 4, pp. 2427–2433, April 2012

[5] Anita Pettersson, Maria Zevenhoven, Britt-Marie Steenari, Lars-Erik Åmand, "Application of chemical fractionation methods for characterisation of biofuels, waste derived fuels and CFB co-combustion fly ashes," Fuel, Volume 87, Issues 15–16, pp. 3183–3193, 2008.

[6] Eduardo Ferrer, Martti Aho, Jaani Silvennoinen, Riku-Ville Nurminen, "Fluidized bed combustion of refuse-derived fuel in presence of protective coal ash," Fuel Processing Technology, Volume 87, Issue 1, pp. 33–44, 2005.

[7] Manninen H., Peltola K. ,Ruuskanen J., "Co-combustion of refuse-derived and packaging-derived fuels (RDF and PDF) with conventional fuels," Waste Management and Research, Volume 15, Issue 2, pp. 137–147, 1997.

[8] Kim DW., Lee JM., Kim JS.,"Co-Combustion of Refuse Derived Fuel with Anthracites in a CFB Boiler," Proceedings of the 20th International Conference on Fluidized Bed Combustion. Springer, Berlin, Heidelberg, 2009.

[9] Ropp, J.; Stäger, T.; Röthlisberger, R., "XyloChips—Continuous Measurement of Woodchips Energy Content," Holzenergie-Symposium Netzintegration, Vorschriften und Feuerungstechnik, Zürich, Switzerland, 2018.

[10] Meiller, M.; Oischinger, J.; Daschner, R.; Hornung, A., "Development of a New Sensor Module for an Enhanced Fuel Flexible Operation of Biomass Boilers," Processes, 9, 661, 2021.

[11] J. Kortela, S.-L. Jämsä-Jounela, "Fuel-quality soft sensor using the dynamic superheater model for control strategy improvement of the BioPower 5 CHP plant," International Journal of Electrical Power & Energy Systems, Volume 42, Issue 1, 2012.

[12] Striugas, N.; Vorotinskiene, L.; Paulauskas, R.; Navakas, R.; Džiugys, A.; Narbutas, L., "Estimating the fuel moisture content to control the reciprocating grate furnace firing wet woody biomass," Energy Convers. Manag., 149, 937—949, 2017.

[13] E. Ikonen, J. Kovacs and J. Ritvanen, "Circulating fluidized bed hot-loop analysis, tuning and state-estimation using particle filtering," International Jounal of Innovative Computing, Information and Control, vol. 9, nro 8, 3357–3376, 2013.

[14] J. Ritvanen, J. Kovacs, M. Salo, M. Hultgren, A. Tourunen and T. Hyppänen, "1-D dynamic simulation study of oxygen fired coal combustion at pilot scale CFB boiler," The 21st International Conference on Fluidized Bed Combustion, Naples, Italy, 2012.

[15] M. Verhaegen and P. Dewilde, "Subspace Model Identification Part 1. The Output-Error State-Space Model Identification Class of Algorithms," Int Journal of Control, vol. 56, no. 5, pp. 1187-1210, 1992.

[16] Tohru Katayama, "Subspace methods for system identification," Vol. 1, London: Springer, 2005.